Progress In Electromagnetics Research Letters, Vol. 100, 127–135, 2021

A Low-Profile Wideband BPF for Ku Band Applications

Ambati Navya*, Govardhani Immadi, and Madhavareddy V. Narayana

Abstract—A low-profile, compact size and light weight wide band BPF prototype is presented for satellite communication applications (Ku-band). The proposed wideband BPF satisfies the International Telecommunication Union's (ITU) region 3 spectrum requirement. Direct broadcast service (DBS) and fixed satellite service (FSS) in transmitting mode respectively employ the frequency band 11.41–12.92 GHz. The proposed filter offers an impedance bandwidth of 1.5 GHz and group delay of 0.2 ns. The proposed wideband BPF is fabricated, and various parameters such as return loss, insertion loss, phase delay, and group delay are measured. Miniaturization of filter size reveals the filter's suitability to use on smaller platforms with smaller surfaces.

1. INTRODUCTION

ITU divided the world into three zones for satellite applications in order to efficiently organize spectrum. The frequency bands for fixed satellite service (FSS) in receiving and transmitting modes in region-3 are 12.2 to 12.7 GHz and 14 to 14.5 GHz, respectively. The reception and transmission frequencies for direct broadcast service (DBS) are 11.7 to 12.2 GHz and 17.3 to 17.8 GHz, respectively. The proposed structure meets the region-3 spectrum requirement for FSS and DBS in transmitting mode. One of the major challenges in the telecommunications system is spectral efficiency. Because spectrum is both scarce and important, it should be used efficiently, which requires the transceiver to be designed to match the criteria. Adaptive devices such as antennas [1], filters, couplers [2], power dividers, and other devices have been developed as a result. Channel selection relies heavily on microwave filters. In order to achieve optimal spectrum utilization, which involves the use of wireless communication systems, it is required to focus on the development and implementation of planar microstrip filters. Due to its efficiency in suppressing interference and noise signals, microstrip bandpass filters (BPFs) are widely utilized in a variety of applications, primarily in Radio frequency and Microwave wireless communications [3, 4]. Microstrip BPFs are used to suppress harmonic signals in fourth-generation (4G) and 5G applications [5–8]. The number of zeroes, poles, input and output external quality factors, coupling coefficients, and resonator configuration are critical characteristics that define the filter performance in microstrip BPFs [9]. Several design strategies, such as the stepped-impedance resonator (SIR), combline, coupled-line, open-ring and stub impedance filters have been presented in the literature [11–15]. BPFs are represented by using lumped elements, waveguides, split ring resonators, microstrip transmission lines, and parallel coupled lines. If the filters are simulated by using the above defined, lumped elements are difficult to fabricate at microwave frequencies; waveguides will occupy more space; split resonators have more circuit losses; parallel coupled lines will have large size and poor selectivity. The most significant feature is compact size employing quarter wavelength transmission lines rather than half wavelength transmission lines which will result in a lower dimension. If we use these microstrip transmission lines to represent filters, circuits will have low losses, a small size, light weight, and easy implementation. Even though lumped element filters are simple to use and efficient,

Received 21 August 2021, Accepted 24 September 2021, Scheduled 19 October 2021
* Corresponding author: Ambati Navya (ambatinavya88@gmail.com).
The authors are with the Department of ECE, KLEF, Vaddeswaram, Guntur, Andhra Pradesh, India.

they are difficult to manufacture at microwave frequencies. As a result, researchers are working on converting distributed element circuits to microwave circuits and vice versa. The intent of the designers is to find a direct transformation method for microstrip filters, such as Richard's transformations, Kuroda's identities, impedance and admittance inverters. These transformations are particularly used in microstrip low pass filters, stopband filters and bandpass filters. Because of the complexity of the layouts, certain types of BPF are not described with their equivalent lumped element circuits in the literature.

We proposed a low-profile, small-size, light-weight filter to meet the ITU's requirement for wideband operation (transmitting mode for FSS and DBS services). These requirements are not met by any of the filters mentioned above. Furthermore, the defined wideband BPF design is simple, easy to integrate and implement. The work is categorised as follows: Part 1 contains an introduction and a literature review. Part 2 contains a detailed overview of the design. Part 3 explains the results, and Part 4 wraps up the proposed work.

2. DETAILS OF THE PROPOSED FILTER DESIGN

A uniform impedance resonator is proposed to adapt to the confined space, and it inherits the calculation theory, as depicted in Figure 1. Its equivalent circuit diagram is presented in Figure 2. The relation among electrical length, width W, and resonant frequency of the uniform impedance resonator is described as follows after determining the microstrip substrate parameters.

$$L = \frac{\lambda_g}{4} \tag{1}$$

$$\lambda_g = \frac{\lambda_0}{F_r \sqrt{E_{r_{eff}}}} \tag{2}$$

F_r is the resonant frequency, where λ_g is the guided wavelength, and the length of the resonator is one-fourth of the guided wavelength. As microstrip is a fundamental structure, the effective dielectric constant and w/h are calculated using the formulae below.

$$\varepsilon_{reff} = \frac{\varepsilon_r + 1}{2} + \frac{\varepsilon_r - 1}{2}\left[1 + \left[\frac{12h}{w}\right]\right]^{-1/2} \tag{3}$$

$$\frac{w}{h} = \frac{2}{n}\left\{(B-1) - \ln(2B-1)\frac{E_r - 1}{2E_r}\left[\ln(B-1) + 0.39 - \left(\frac{0.61}{2E_r}\right)\right]\right\} \tag{4}$$

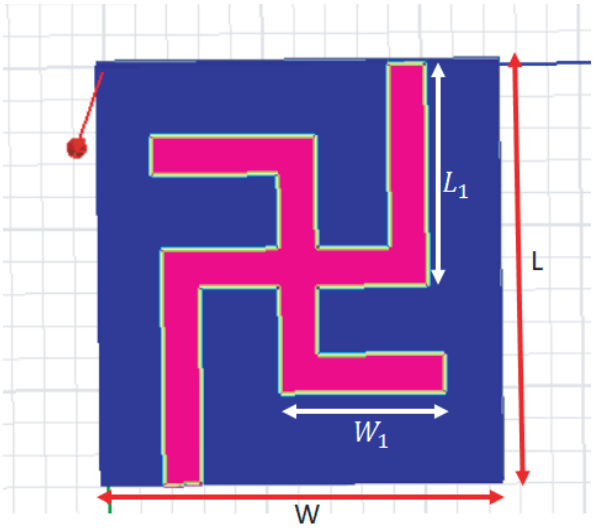

Figure 1. Schematic diagram of the wide band BPF.

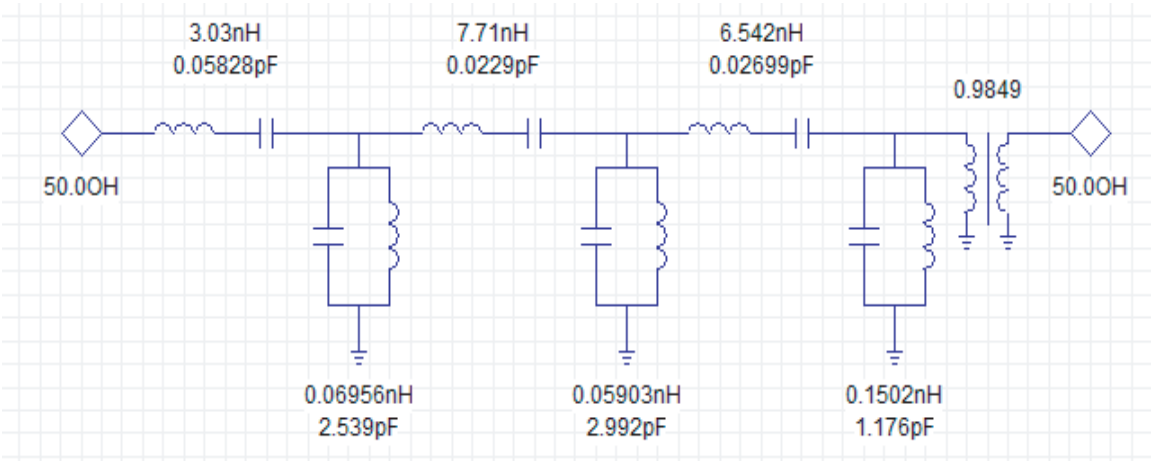

Figure 2. Equivalent circuit diagram.

$$B = \frac{60^2}{Z_{C\sqrt{\varepsilon_r}}} \tag{5}$$

W is the resonator's width, h the grounded dielectric substrate's thickness, and ε_r the substrate's dielectric constant. When the W/h ratio exceeds one, the substrate used in this paper meets this condition. The bandwidth of the proposed design is increased by positioning the $\lambda/4$ transmission line in such a way that it provides the desired shape, and only the equivalent circuit diagram is constructed based on that shape. A series LC circuit is formed when $\lambda/4$ transmission lines are connected in series; otherwise, a shunt LC circuit is formed.

According to the calculation theory, f_r may be changed by changing L or W, and when one of these two variables is constant, increasing the other causes f_r to drop. The simulation results confirm the forecast results based on the theoretical Equation (4) and Equations (1)–(3).

The proposed wideband BPF shown in Figure 1 comprises four $\lambda/4$ transmission lines and two 50-Ohm feed lines to connect the resonating lines. The coupling or external quality factor of the microstrip resonators is controlled by the tapping position t. The smaller the t is, the weaker the relationship is, or the higher the external quality factor is [1]. The proposed wideband BPF was simulated using Ansoft HFSS software, and the BPF was designed using FR4 material with a thickness of 1.6 mm. The dimensions of the simulated wideband BPF are shown in Table 1. The proposed filter's design

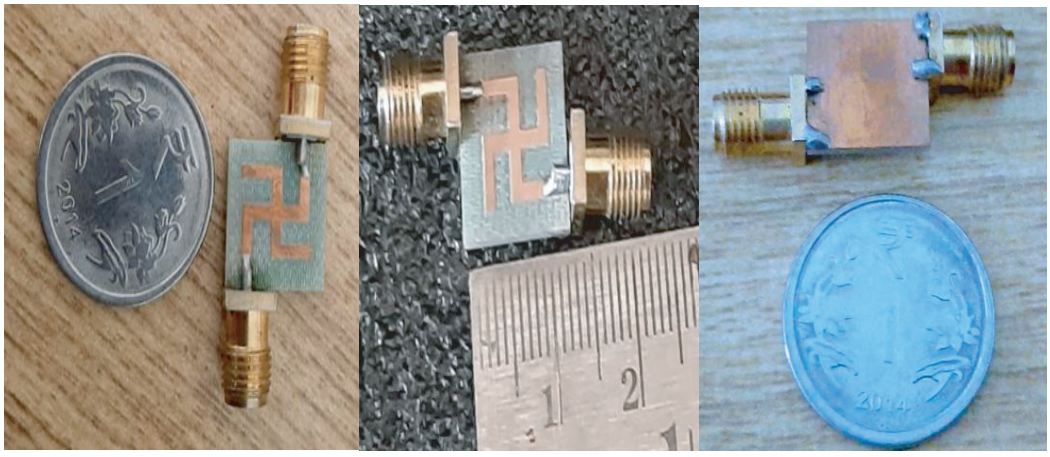

(a) (b) (c)

Figure 3. Photographs of the manufactured wideband BPF from side, top and bottom.

Table 1. Dimensions for wideband BPF.

Parameters	L	W	L_1	W_1
Dimensions (mm)	12.5	13	6	2

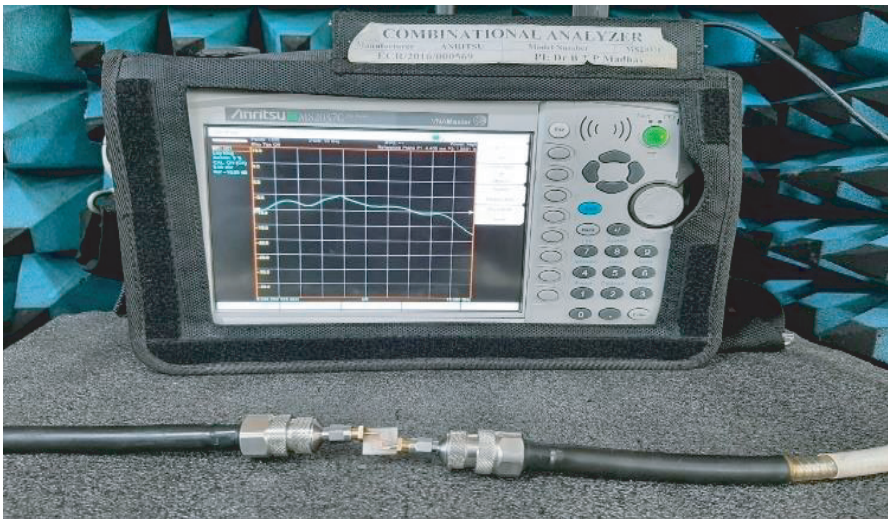

Figure 4. Measuring the transmission coefficient by using combinational analyser.

dimensions are shown in Figure 1, and the manufactured filter is shown in Figure 3. Figure 4 presents the measurement of a transmission coefficient by using Anritsu combinational analyser and the parameters measured by using this combinational analyser are S-parameters, group delay, and phase delay.

3. RESULTS

Chemical etching is used to fabricate the defined wideband BPF without defective ground structures (DGSs) or vias, and two SMA connectors are utilised to connect the I/O lines and ground, as depicted in Figure 3. The size of the fabricated wideband BPF is 12.5×13 mm, with λ_g being the guided wavelength at the desired frequency of the passband. The fabricated wideband BPF is attached to the combinational analyser (Anritsu MS2037C) through SMA connectors in order to measure the S-parameters.

Figures 5 and 6 depict the simulated and measured S_{11}, S_{12} responses of the wideband BPF. Figure 7 presents the simulated and measured responses, and Figure 8 indicates S_{11} and S_{21} responses of wideband BPF having a transmission zero at 15 GHz. The designed wideband BPF has a passband with a center frequency of 12 GHz and a 3-dB fractional bandwidth (FBW) of 12.5 percent, according to the measured results. At the resonant frequency, the passband has an insertion loss of 0.2 dB and a reflection coefficient of 18 dB. Between the passband and transmission zero, which is positioned at 15 GHz, there

Table 2. Comparison of simulated results of wideband BPF with fabricated results.

Parameters	Simulated	Fabricated
Return loss	−16.56 dB	−15.56 dB
Insertion loss	−0.2 dB	−0.6 dB
Group delay	0.2 ns	0.6 ns
Band width	1.5 GHz	1.2 GHz

is an increase in band-to-band isolation and out-of-band rejection. Due to manual alignment, cable and connection losses and higher mode excitation, minor differences between the simulated and manufactured results are observed.

Figure 9 indicates the E-field, H-field, and current distributions of the filter at resonant frequency, i.e., 12 GHz, and from the current distribution it is observed that a peak value of current at the feed lines is $1.8 \times e^2$ Amp/meter. The arrow sign is used to show in which way the current is flowing. The current distribution, on the other hand, appears almost regular at different parts of the wideband BPF. The wideband BPF has effective signal selection performance for the propagated signal, according to the simulation results of the electric field distributions.

The proposed wideband filter attains a group delay of 0.2 ns throughout the passband as shown in Figure 10. This indicates that in this duration the phase change of the signal remains linear. Figure 10 shows that the group delay is not constant throughout the frequency range, and at the

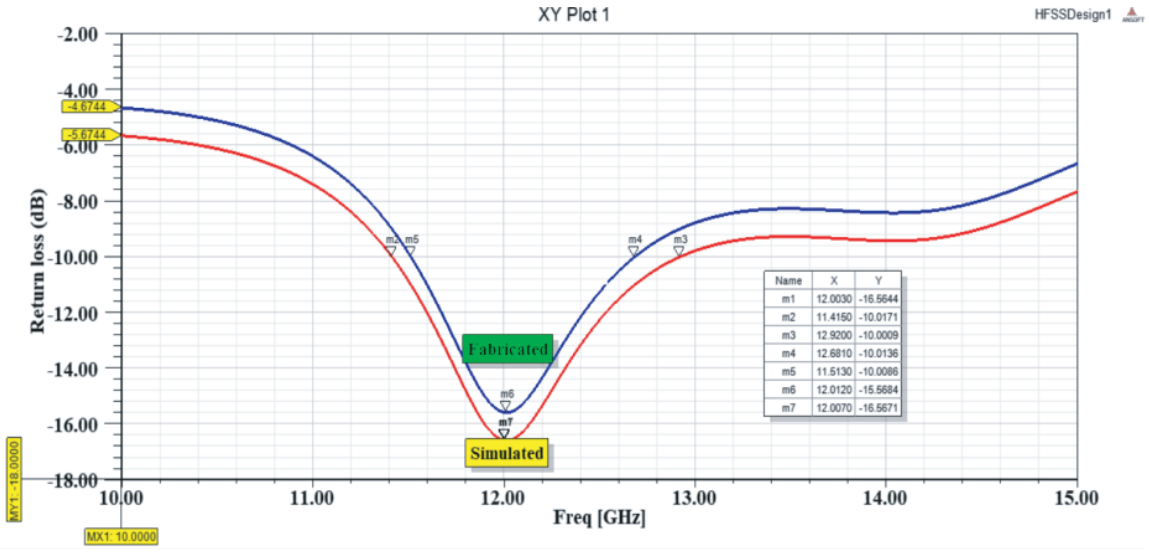

Figure 5. Simulated and fabricated S_{11} response of wideband BPF.

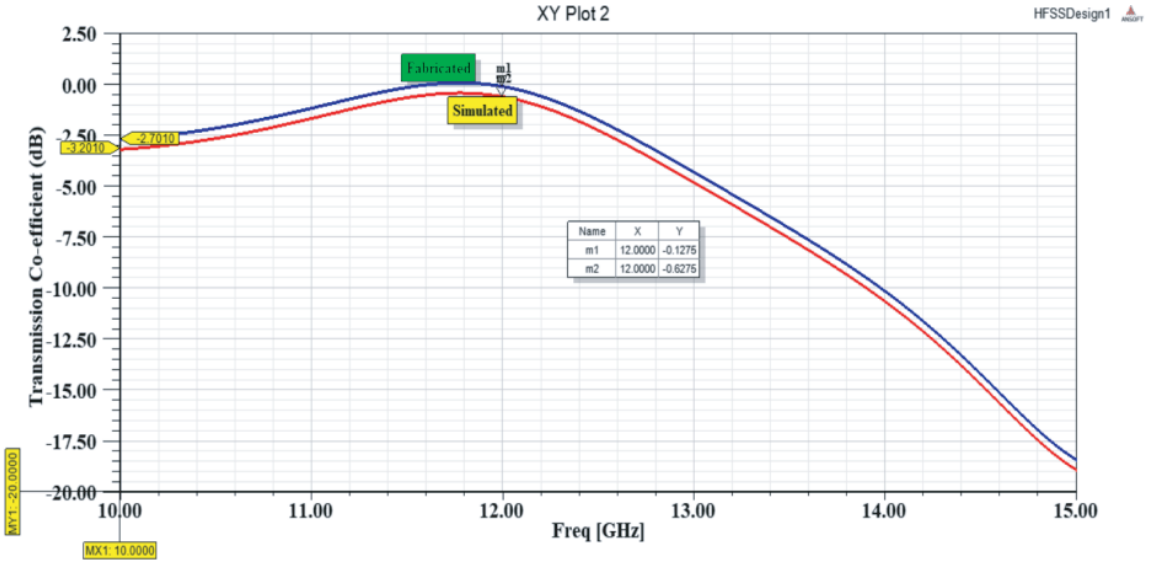

Figure 6. Simulated and fabricated S_{12} response of wideband BPF.

resonant frequency the group delay is less than 1 ns, with simulated and manufactured delays of 0.2 ns and 0.6 ns, respectively. Figure 11 shows that phase changes with frequency are smooth and that there is no inconsistency in phase change inside the BPF's pass band.

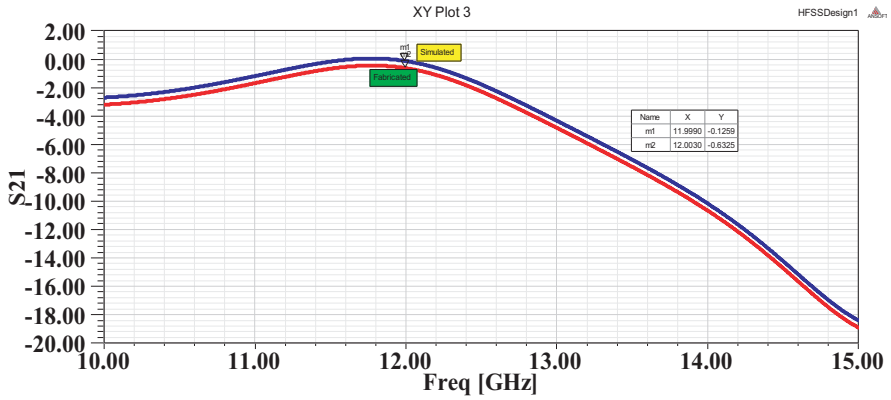

Figure 7. Simulated and fabricated S_{21} response of wideband BPF.

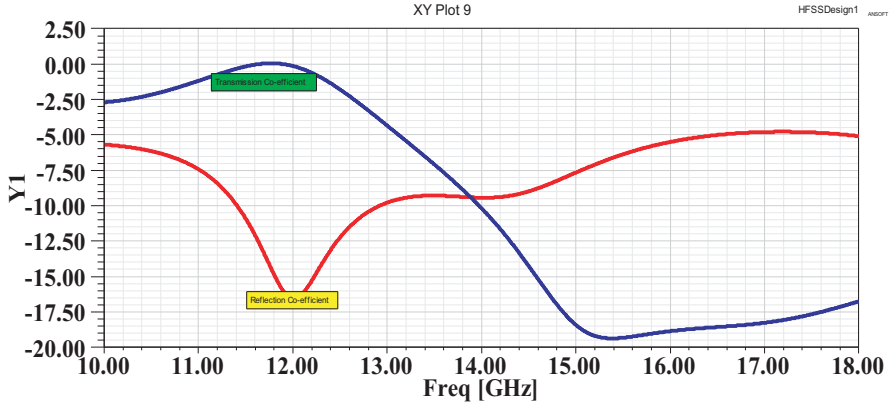

Figure 8. S_{11} and S_{21} response of wideband BPF having a transmission zero at 15 GHz.

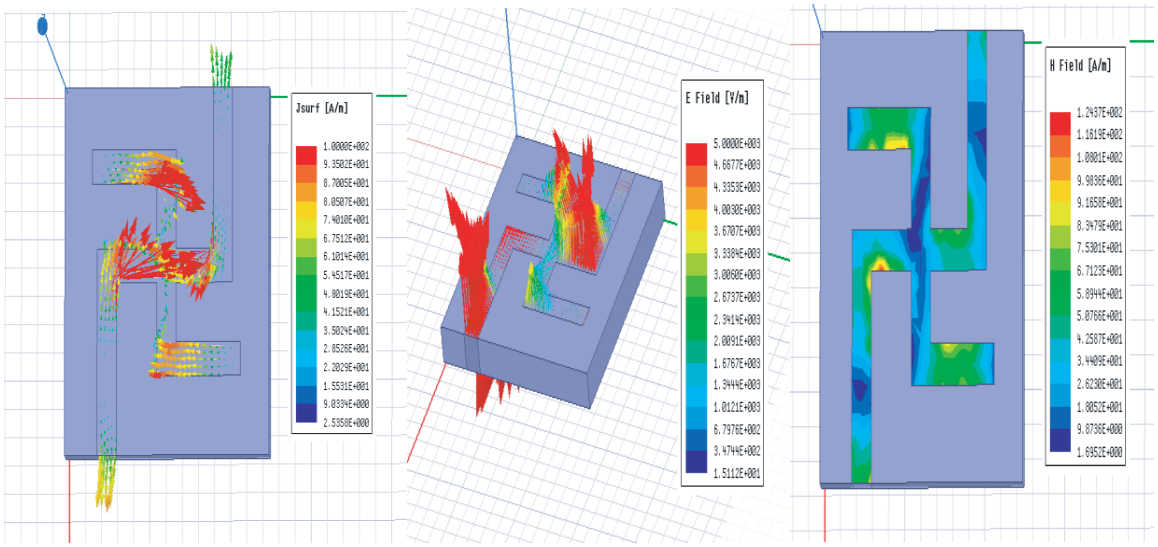

Figure 9. E-field, H-field, and Current distributions of wide band BPF.

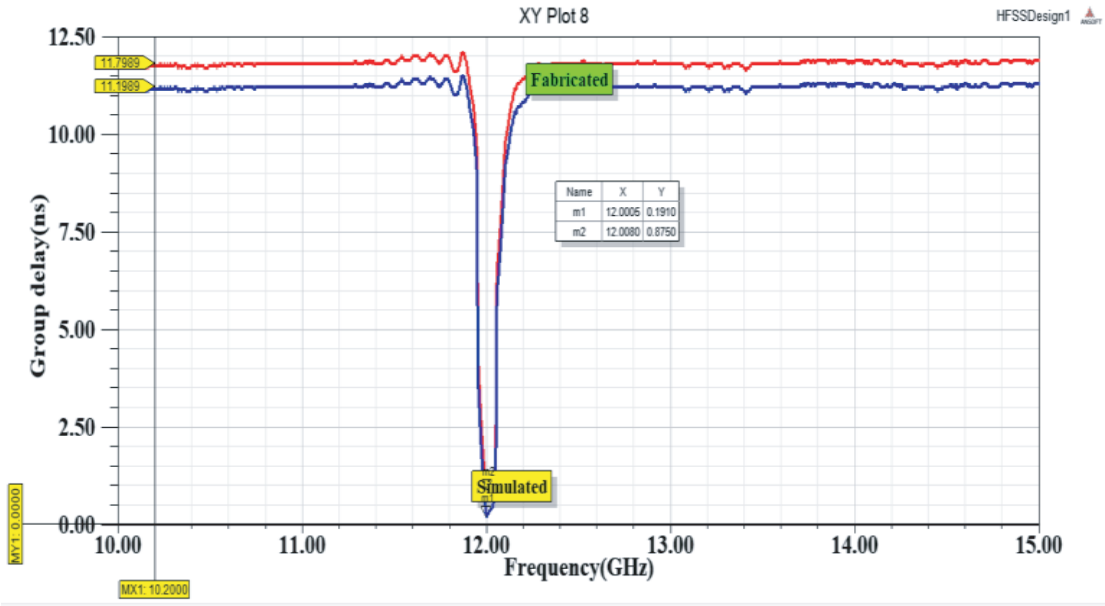

Figure 10. Group delay of the wide band BPF.

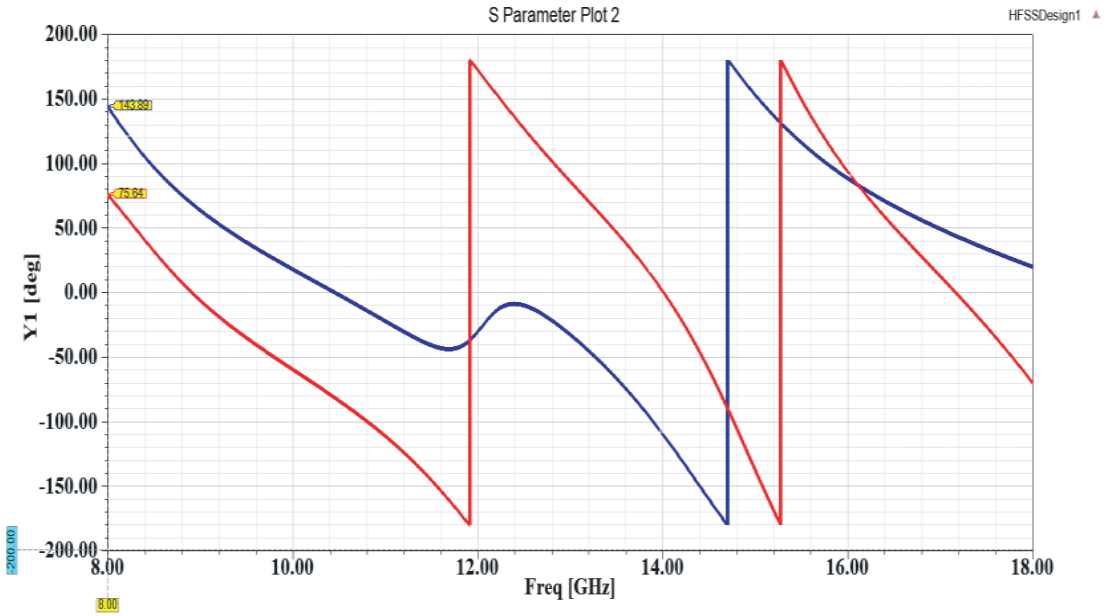

Figure 11. Phase delay of the wide band BPF.

Table 2 shows the comparison of simulated results of wideband BPF with fabricated results for various parameters such as return loss, insertion loss, group delay, and bandwidth. Table 3 compares the proposed wideband BPF in this article to various mentioned wide band BPFs at Ku band in terms of its outcomes. Furthermore, among the equivalents, the insertion losses remain the lowest. When the results are observed, it is evident that the wideband BPF presented in this study has better bandwidth and insertion loss. Filters at Ku band for satellite applications have been proposed in the literature [8–11], but they all have narrower bandwidth and higher insertion loss. The wideband BPF presented in this paper is compared with the bandpass filter proposed in [11] having high return loss; however, the BPF has a bigger size and narrower bandwidths. Chemical etching microstrip devices without DGSs or vias also reduces process costs and improves manufacturing efficiency.

Table 3. Comparison of wideband BPF with the other filters at Ku band.

Design Proposed by	Substrate	Return loss	Insertion loss	Group delay	Area (mm^2)	Center Frequency	Bandwidth	Size in terms of λ_g
[8]	Rogers RT /duroid	−14 dB	−2 dB	-	5×13	13.3 GHz	0.5 GHz	$1.5\lambda_g \times 1.8\lambda_g$
[9]	GaAs	−15 dB	−2.6 dB	-	1.09×0.97	13.5 GHz	0.4 GHz	$1.32\lambda_g \times 1.2\lambda_g$
[10]	FR4	−16 dB	−3 dB	0.234 ns	11.12×8	14 GHz	0.2 GHz	$0.99\lambda_g \times 1.0\lambda_g$
[11]	FR4	−17 dB	−10 dB	-	25×25	10 GHz	1 GHz	$1.56\lambda_g \times 1.4\lambda_g$
Proposed Filter	FR4	−16.56 dB	−0.2 dB	0.2 ns	12.5×13	12 GHz	1.5 GHz	$0.919\lambda_g \times 0.955\lambda_g$

4. CONCLUSION

A wideband BPF with microstrip feed line has been designed for Ku band satellite applications. The proposed wideband BPF is designed for low transmission coefficient, steep passband edges, high out of band rejection, and wide bandwidth, with the frequency band covering the transmitting mode of FSS and DBS services (ITU region-3) with an insertion loss of 0.2 dB and group delay of 0.2 ns. In addition, the proposed filter is the first in this field to offer a short group delay and a large bandwidth, meeting ITU Region 3 standards.

5. FUTURE SCOPE

In future this filter structure can be extended by using additional features like via-hole and defected ground structure.

REFERENCES

1. Hong, J. S. and M. J. Lancaster, *Microstrip Filters for RF/Microwave Applications*, Vol. 167, John Wiley and Sons, Hoboken, NJ, USA, 2004.
2. Richard, J. C., M. K. Chandra, and R. M. Raafat, *Microwave Filters for Communication Systems Fundamentals, Design and Applications*, John Wiley and Sons, Hoboken, NJ, USA, 2017.
3. Ian, H., *Theory and Design of Microwave Filters*, IET Electromagnetic Waves Series 48, IET, London, UK, 2006.
4. Al-Yasir, Y. I. A., N. Ojaroudi Parchin, A. M. Abdul Khaleq, M. S. Bakr, and R. A. Abd-Alhameed, "A survey of differential-fed microstrip bandpass filters: Recent techniques and challenges," *Sensors*, 2356, 2020.
5. Hou, Z., C. Liu, B. Zhang, and R. Song, "Dual-/Tri-wideband bandpass filter with high selectivity and adjustable passband for 5G mid-band mobile communications," *Electronics*, 205, 2020.
6. Guan, Y., Y. Wu, and M. M. Tentzeris, "A bidirectional absorptive common-mode filter based on interdigitated microstrip coupled lines for 5G green communications," *IEEE Access*, 20759–20769, 2020.
7. Al-Yasir, Y. I. A., N. O. Parchin, A. Abdul Khaleq, K. Hameed, M. Al-Sadoon, and R. Abd-Alhameed, "Design, simulation and implementation of very compact dual-band microstrip bandpass filter for 4G and 5G applications," *Proceedings of the 16th International Conference on Synthesis, Modelling, Analysis and Simulation Methods and Applications to Circuit Design (SMACD)*, 41–44, Lausanne, Switzerland, July 2019.

8. Yang, Q., X. Xiong, Y. Wu, L. Wang, and H. Xiao, "Design of microstrip tapped-hairpin dual-band pass filter for Ku-band application," *2010 International Conference on Microwave and Millimeter Wave Technology*, 772–774, Chengdu, 2018.
9. Sheen, J., Y. Cheng, and W. Liu, "Ku-band bandpass filter design with compact size and broad stopband by pHEMT process," *2019 Photonics & Electromagnetics Research Symposium — Spring (PIERS — Spring)*, 1022–1026, Rome, Italy, June 17–20, 2019.
10. Panda, C. S., R. Nayak, and S. K. Behera, "Design and analysis of a compact Substrate Integrated Waveguide bandpass filter for Ku band applications," *2016 Online International Conference on Green Engineering and Technologies (IC-GET)*, 1–5, Coimbatore, 2020.
11. Ghatak, R., P. Sarkar, R. K. Mishra, and D. R. Poddar, "A compact UWB bandpass filter with embedded SIR as band notch structure," *IEEE Microwave Wireless Component Letters*, 261–263, 2011.
12. Liu, H., T. Liu, Q. Zhang, B. Ren, and P. Wen, "Compact balanced bandpass filter design using asymmetric SIR pairs and spoof surface plasmon polariton feeding structure," *IEEE Microwave Wireless Component Letters*, 987–989, 2018.
13. Yuceer, M., "A reconfigurable microwave combline filter," *IEEE Transactions on Circuits Systems II Express Briefs*, 84–88, 2016.
14. Cho, Y., H. Baek, H. Lee, and S. Yun, "A dual-band combline bandpass filter loaded by lumped series resonators," *IEEE Microwave Wireless Component Letters*, 626–628, 2009.
15. Velez, P., J. Naqui, A. Fernandez-Prieto, M. Duran-Sindreu, J. Bonache, J. Martel, F. Medina, and F. Martin, "Differential bandpass filter with common-mode suppression based on open split ring resonators and open complementary split ring resonators," *IEEE Microwave Wireless Component Letters*, 22–24, 2013.